Comparison of homogeneous and heterogeneous electrochemical advanced oxidation processes for treatment of textile industry wastewater

Sié Alain Hien, Clément Trellu, Nihal Oturan, Alain Stéphane Assémian, Bi Gouessé Henri Briton, Patrick Drogui, Kopoin Adouby, Mehmet Oturan

Comparison of homogeneous and heterogeneous electrochemical advanced oxidation processes for treatment of textile industry wastewater

Sié Alain Hien[1,2], Clément Trellu[1,*], Nihal Oturan[1], Alain Stéphane Assémian[3], Bi Gouessé Henri Briton[2], Patrick Drogui[4], Kopoin Adouby[2], Mehmet A. Oturan[1,*]

[1] Université Gustave Eiffel, Laboratoire Géomatériaux et Environnement EA 4508, 77454 Marne-la-Vallée, Cedex 2, France.

[2] Laboratoire des Procédés Industriels, de Synthèse de l'Environnement et des Energies Nouvelles (LAPISEN), Institut National Polytechnique Houphouët-Boigny, BP 1313 Yamoussoukro, Côte d'Ivoire.

[3] Laboratoire de Thermodynamique et Chimie Physique de l'Environnement, Université de Nangui-Abrogoua, 02 BP 801 Abidjan 01, Côte d'Ivoire.

[4] INRS Eau, Terre et Environnement, 490, rue de la Couronne, Québec G1K9A9, Canada

Manuscript submitted to **Journal of Hazardous Materials** for consideration

Corresponding authors' Eùails:

mehmet.oturan@univ-eiffel.fr (Mehmet A. Oturan)

clement.trellu@univ-eiffel.fr (Clément Trellu)

Abstract

This study aimed at understanding the influence of the generation of oxidants in a heterogeneous way at boron-doped diamond (BDD) anode (anodic oxidation (AO)) or homogeneously in the bulk (electro-Fenton (EF)) during treatment of a textile industry wastewater. Both processes achieved high TOC removal. A yield of 95% was obtained by combining EF with BDD anode during 6 h of treatment. The EF process was found to be faster and more efficient for discoloration of the effluent, whereas AO was more effective to limit the formation of degradation by-products in the bulk. An advantage of AO was to treat this alkaline effluent without any pH adjustment. Operating these processes under current limitation allowed optimizing energy consumption in both cases. However, using BDD anode led to the formation of very high concentration of ClO_3^-/ClO_4^- from Cl^- oxidation (even at low current density), which appears as a key challenge for treatment of such effluent by AO. By comparison, EF with Pt anode strongly reduced the formation of ClO_3^-/ClO_4^-. Operating EF at low current density even maintained these concentrations below 0.5% of the initial Cl^- concentration. A trade-off should be considered between TOC removal and formation of toxic chlorinated by-products.

Keywords: Anodic Oxidation, Electro-Fenton, Mineralization, Dye, Perchlorate

1. Introduction

Effluents from textile and tannery industry contain large amounts of dyes [1–3]. The discharge of such effluents in the environment presents several critical drawbacks, including the impact on the color of water bodies and critical effects related to the acute and long-term toxicity of some dyes [4]. The textile industry consumes more than 10 billion liters of water per day as well as 800 000 tons of dyes, of which 120 000 tons end up in wastewaters [4]. These very specific effluents contain high concentrations of dyes as well as other organic and mineral compounds depending on the dyeing process. Biological treatments are usually not suitable because of the low biodegradability of dyes, low N content, high salinity and high pH of these effluents [5]. Strong adverse effects were also observed from the discharge of these effluents in municipal wastewater due to their toxic effects on the biomass of conventional activated sludge process [6]. Therefore, advanced processes have to be developed for on-site treatment of these hazardous effluents [5,7].

Coagulation and electro-coagulation have been widely studied for the treatment of textile wastewater [7,8]. For example, electro-coagulation was able to remove 99% of turbidity but only 79% of chemical oxygen demand (COD) from a textile industry effluent (not enough for meeting environmental standards) [1]. Moreover, such treatment involves only a transfer of pollutants from the liquid to the solid phase and the generated sludge represents an additional waste to manage. Conventional oxidation processes using ozone or Fenton process have also been applied. While the removal of the color is very fast, an important issue is usually related to the recalcitrance of some degradation by-products [9–12]. A pH adjustment step is also often required for optimization of these processes [13,14].

Electrochemical advanced oxidation processes (EAOPs) are emerging processes presenting a crucial advantage related to their non-selectivity for the full mineralization of organic pollutants [15–22]. They are based on the generation of hydroxyl radicals (•OH), the second

most powerful oxidant known [23]. Electro-Fenton (EF) and anodic oxidation (AO) are the two most popular EAOPs [15]. The AO process is based on the generation of $^{\bullet}OH$ from water oxidation (Eq. 1) at the surface of anode material with high overpotential for oxygen evolution reaction [24,25]. Other oxidant species can also be generated depending on electrode materials and ions in the solution. For example, active chlorine and persulfates can be generated in effluents containing Cl^- and SO_4^{2-} ions [15]. The EF process is based on the formation of $^{\bullet}OH$ from electrochemical generation of the Fenton's reagent (Fe^{2+} and H_2O_2) (Eq. 2) by (i) the two electron reduction of dissolved O_2 on carbonaceous cathode materials and (ii) the one electron reduction of Fe^{3+} to Fe^{2+} at the cathode [26,27]. By using a suitable anode material, formation of $^{\bullet}OH$ at the surface of the anode can also enhance the oxidation power of the EF process [18,28].

$$M + H_2O \rightarrow M(^{\bullet}OH) + H^+ + e^- \quad (1)$$

$$Fe^{2+} + H_2O_2 \rightarrow Fe^{3+} + {}^{\bullet}OH + OH^- \quad (2)$$

Several studies have reported the possibility to use EAOPs for the degradation and mineralization of a large range of organic compounds, including dyes [7,29–32]. However, there is a lack in treatment of real wastewaters by EAOPs [33]. Therefore, further development of EAOPs still requires addressing several challenges such as (i) the optimization of the process for a specific application, (ii) the understanding of reaction mechanisms in complex real effluents and (iii) the evaluation of the formation of toxic by-products generated during the process [15,20,34]. Particularly, it is important to well understand the different advantages and drawbacks of the different EAOPs. The $^{\bullet}OH$ are generated in a different way during AO and EF. They are homogeneously generated in the bulk solution in the EF process, while they are generated and accumulated at the surface of the anode in the AO process [16,18,22,25,35]. Therefore, the aim of this study was to compare AO and EF processes for the treatment of a real effluent from the textile industry.

The different behaviors in terms of degradation and mineralization kinetics of organic compounds were emphasized. Moreover, the evolution of chlorate (ClO_3^-) and perchlorate (ClO_4^-) generated from oxidation of chloride was monitored since it is an important issue that should be further taken into consideration for integration of EAOPs in a real wastewater treatment system.

2. Material and methods

2.1 Chemicals

All chemicals were HPLC or analytical grade. Sulfuric acid (98%) and nitric acid (65%) were provided from Fluka. Chemical reagents for determination of chemical oxygen demand (COD) were obtained from Sigma Aldrich (K_2CrO_7 and Ag_2SO_4) or Merck (Hg_2SO_4). Iron (II) sulfate heptahydrate ($FeSO_4 \cdot 7H_2O$, 99.9%) and potassium hydrogen phthalate ($C_8H_5KO_4$, 99.95%) were obtained from Merck. Dilutions and solutions were prepared with ultra-pure water produced by a Milli-Q system (resistivity > 18.2 MΩ cm at 25 °C). The dye wastewater was obtained from a textile industry in Ivory Coast. Various dyes were provided by the textile industry in order to identify the main dye contained in the effluent.

2.2 Electrochemical reactor

An undivided cylindrical open batch reactor was used for performing electrochemical processes. The total volume of the treated solution was 230 mL and it was maintained under continuous magnetic agitation. Experiments were performed under galvanostatic conditions using a DC power supply (Hameg, HM8040-3).

For the AO process, plate electrodes were placed face to face with an inter-electrode distance of 2 cm. The anode was a boron-doped diamond (BDD) thin film deposited onto a niobium (Nb) substrate from Condias (6 × 4 cm^2), while the cathode was stainless steel AISI 304

obtained from Goodfellow (6 × 4 cm^2). The influence of the solution pH (3, 8 and 13.4) of the effluent was studied by adjustment of the initial pH with sulfuric acid.

For the EF process, a carbon felt obtained from Mersen (16 × 5 cm^2) was used as cathode and placed on the inner wall of the cylindrical reactor. The anode was placed at the center of the reactor, using either a Pt (noted EF/Pt process) or a BDD anode (noted EF/BDD process). A concentration of 0.1 mM of iron (II) was added to the solution as catalyst (since iron was not present in the raw effluent) and air was continuously bubbled in the solution in order to provide sufficient dissolved oxygen for production of hydrogen peroxide at the cathode. This reactor setup was similar to the one reported in previous studies [21,22,28,36]. All EF experiments were performed at initial pH of 3 (adjusted with sulfuric acid) in order to avoid precipitation of iron.

The conductivity of the effluent was sufficient to perform the EAOPs without addition of any additional salt.

Experiments were repeated twice and mean values were used to build the graphs.

2.3 Total organic carbon (TOC) analysis

TOC analyses were performed in order to monitor the mineralization rate of the organic matter of the treated solution. Analyses were carried out using a TOC-L from Shimadzu with the non-purgeable organic carbon method. Calibration was performed using potassium hydrogen phthalate in the range 0.20 – 20 mg L^{-1}. Analyses were repeated 2 times, or 3 times if the coefficient of variation was above 2.0%.

2.4 Chemical oxygen demand (COD) analysis

Samples were mixed with the digestion solution (containing K_2CrO_7, H_2SO_4, Ag_2SO_4 and Hg_2SO_4) and incubated at 148 °C for 2 h in a Spectroquant® TR 420 digester (Merck). Analysis was then performed using a Spectroquant® Nova 60 photometer (Merck).

2.5 Current efficiency and energy consumption

Current efficiency (CE_{COD}) for COD removal was calculated using the Eq. 3.

$$CE_{COD}\ (\%) = \frac{(COD_0 - COD_t)\ F\ V}{8\ I\ t} * 100 \quad (3)$$

where COD_0 is the initial COD (mg L^{-1}), t is the treatment time (s), COD_t is the COD at time of treatment t, I is the current intensity (A), V is the volume of the solution (L) and F is the Faraday constant.

Current efficiency for Cl^- oxidation to ClO_3^- and ClO_4^- (CE_{ClOx}) was calculated using the Eq. 4.

$$CE_{ClOx}\ (\%) = \left(\frac{6\ [ClO_3^-]\ F\ V}{I\ t} + \frac{8\ [ClO_4^-]\ F\ V}{I\ t}\right) * 100 \quad (4)$$

where $[ClO_3^-]$ and $[ClO_4^-]$ are the amount of chlorate and perchlorate generated (in M) and 6 and 8 represents the number of electrons involved in the oxidation of Cl^- to ClO_3^- and ClO_4^-, respectively.

Electrical energy consumption (EC) per kg of TOC removed was calculated according to the Eq. 5.

$$EC\ (kWh\ (kg\ TOC)^{-1}) = \frac{1000\ U\ I\ t}{(TOC_0 - TOC_t)\ V} \quad (5)$$

where U is the cell potential (V) and TOC is the total organic carbon (mg L^{-1}) at time 0 and t (h), respectively.

EC per m^3 of treated water was calculated according to the Eq. 6.

137 $$EC\ (kWh\ m^{-3}) = \frac{U\ I\ t}{V} \quad (6)$$

138 **2.6 UV-vis absorbance analysis**

139 UV-vis absorbance analyses were performed in order to follow the discoloration of the
140 effluent, which indicates the degradation of the dyes. Analyses were performed 668 nm (i.e.
141 maximum of absorbance of the effluent in the visible region). Full UV-vis spectra were also
142 recorded in order to better understand the evolution of the nature of organic compounds
143 during the treatment.

144 **2.7 Ion chromatography**

145 Ion chromatography was used for analysis of the main anions in the effluent (Cl^- and SO_4^{2-}) as
146 well as for monitoring the formation of ClO_3^- and ClO_4^- during the treatment. Analyses were
147 performed with a Dionex ICS-1000 equipped with a conductivity detector DS6, an ASRS 300
148 suppressor, an anionic column AS4A-SC (4 mm × 250 mm) and an injection loop of 25 µL.
149 The mobile phase was 1.8 mM sodium carbonate (Na_2CO_3) and 1.7 mM of sodium
150 bicarbonate ($NaHCO_3$). Elution was carried out in isocratic mode with a flow rate of 2 mL
151 min^{-1}.

152 # 3. Results and discussion

153 **3.1 Characterization of the effluent**

154 The effluent treated in this study was directly sampled from wastewaters of the textile
155 industry TEX-CI Gronfreville located at Bouaké (Ivory Coast). Physicochemical
156 characteristics of the effluent are reported in Table 1 and they are compared to national
157 regulations and recommendations from the World Health Organization. High organic loading

158 and a very alkaline pH make this effluent very difficult to treat by most of the conventional
159 techniques without a pH adjustment.

160 Another important characteristic of this effluent was the high concentrations of sodium,
161 chloride and sulfate ions. They come from the addition of sodium hydroxide (NaOH), sodium
162 chloride (NaCl), sodium hydrosulfite ($Na_2S_2O_4$) and sodium hypochlorite (NaClO) during the
163 various steps of the textile industry (bleaching, mercerization, desizing, dyeing). The presence
164 of these salts resulted in a high conductivity, which was suitable for application of the
165 electrochemical process without further addition of any additional salt.

166 The UV-vis absorbance spectrum of the effluent is presented in Fig. 1. Two significant
167 absorbance peaks were observed in the visible region, at 624 and 668 nm. These peaks are
168 ascribed to the chromophore groups of a dye. The effluent spectrum was then compared with
169 the spectrum of various individual dyes used by the textile industry (Fig. 1 and Fig. SI-1). The
170 comparison allowed for identification of Bezathren Dark Blue (BDB) as the main dye
171 contained in the effluent. Chemical structure of this anthraquinone-based dye is provided in
172 Fig. SI 2; it is an aromatic compound containing two anthraquinone units and two amino
173 (chromophore) groups [37]. Besides, for a similar value of absorption in the visible region, the
174 absorbance of the effluent in the UV region was much higher than for BDB dye. It was
175 ascribed to the presence of organic additives absorbing in the UV region such as detergents,
176 surfactants, binders or thickener used by the textile industry. These results highlight that this
177 kind of effluent is a complex mixture of organic and inorganic compounds that is difficult to
178 treat using conventional treatment methods.

179

180

Table 1 – Main physicochemical characteristics of the textile effluent under study and discharge limitations

Parameters (unit)	**Values**	**National regulation (Ivory Coast)** [(a)]	**World Health Organization**[(b)]
pH	13.40	5.5-9.5	6.5-9.5
Conductivity (mS/cm)	9.31		0.4
COD (gO_2/L)	1.10	0.50	0.25-0.50
TOC (g/L)	0.45		
SS (g/L)	0.15	0.05	0.05
$[Na^+]$ (g/L)	1.07		0.15
$[Cl^-]$ (g/L)	0.44	0.05	0.15
$[SO_4^-]$ (g/L)	0.18		0.5
Color	Blue	Colorless	Colorless

(a) Ivory Coast recommendations for effluent discharge in the environment [38]

(b) World Health Organization recommendation for effluent discharge in the environment [39]

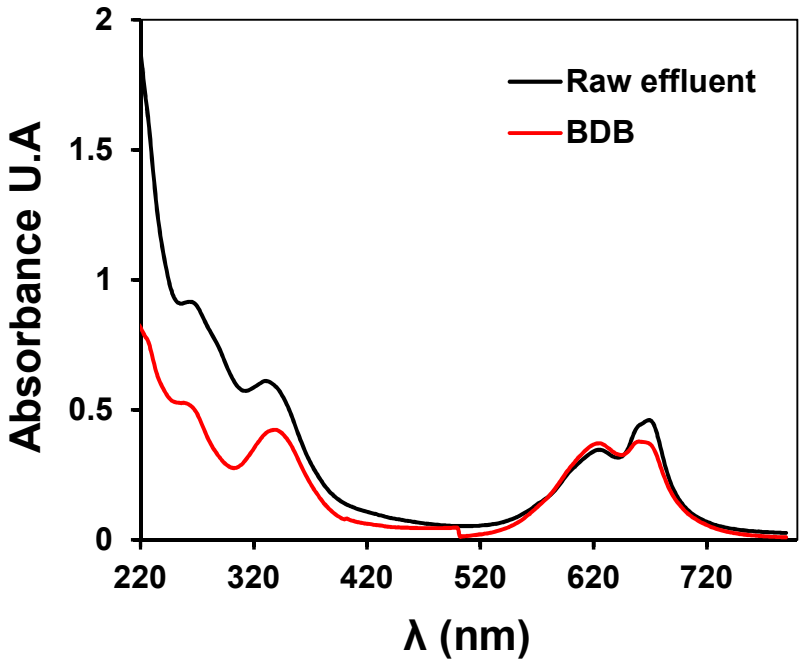

Figure 1 – Comparison of the UV-vis spectrum of raw effluent (black line) and solution of Bezathren Dark Blue (BDB) dye (red line).

3.2 Comparison of EF (homogeneous) and AO (heterogeneous) processes for mineralization of organic compounds in textile wastewater

The first objective of this study was to compare the effectiveness of the different EAOPs (AO with BDD anode (AO/BDD), EF with Pt anode (EF/Pt) and EF with BDD anode (EF/BDD)) for the removal of TOC. The evolution of TOC in the solution was monitored in order to follow the mineralization kinetic of organics in the solution (Fig. 2a). After 6 h of treatment at 200 mA (current density of 8.3 mA cm^{-2}), 52%, 75% and 95% of the initial TOC was removed from the solution by using EF/Pt, AO/BDD and EF/BDD, respectively. The higher efficiency of EF/BDD was explained by formation of a larger amount of $^{\bullet}OH$ coming from both water oxidation at the BDD surface and Fenton's reaction in the bulk. However, it is interesting to notice that $^{\bullet}OH$ are not generated in the same way during EF (homogeneously in

202 the bulk) and AO (heterogeneously at the anode surface) processes. The next objective was
203 therefore to understand the impact on the mineralization kinetics.

204 Linear regression analysis of mineralization kinetics highlighted different behaviors.
205 Mineralization of organic compounds by AO/BDD process clearly followed a pseudo-zero
206 order kinetic (Eq. 8 and Fig. 2b) (k_0 = 50 mg L^{-1} h^{-1}). In this case, $^{\bullet}OH$ are generated and
207 accumulated in a heterogeneous way, only at the surface of the BDD anode [25]. Therefore,
208 this kinetic behavior was explained by the high concentration of organic compounds
209 compared to the current intensity supplied to the system [24,40]. Considering a typical mass
210 transfer coefficient of organic compounds from the bulk to the electrode surface in such batch
211 configuration ($k_m = 3.10^{-5}$ m s^{-1}), the limiting current density (Eq. 7) was calculated as 40 mA
212 cm^{-2} at the beginning of the process [24]. It is also possible to calculate that the process was
213 operated under current limitation as long as the removal rate of COD was below ≈ 80% (i.e.
214 almost during the whole 6 h of treatment). During this period, the reaction rate depends only
215 on current and not on the concentration of organic compounds, thus explaining why a pseudo-
216 zero order kinetic was obtained.

217 $$j_{lim} = 4\,F\,k_m\,COD \qquad (7)$$

218 with j_{lim}, the limiting current density (A m^{-2}); F, the Faraday constant; k_m, the mass transport
219 coefficient (m s^{-1}) and COD, the chemical oxygen demand (mol m^{-3})

220 $$\frac{d\,TOC(t)}{dt} = k_0 \qquad (8)$$

221 with k_0, the pseudo-zero order rate constant

222 By comparison, EF/Pt and EF/BDD processes followed rather a pseudo-first order kinetic
223 (Eq. 9) for the mineralization of organic compounds (Fig. 2c). The mineralization rate
224 depends, in this case, on the concentration of organic matter in the solution. The EF/Pt

process generates •OH in a homogeneous way in the bulk. These •OH have very short lifetime, e.g., the reaction rate between two •OH ($k = 5.5 \times 10^9$ mol s^{-1} L^{-1}) [41] is in the same order of magnitude than the reaction rate between •OH aromatic compounds ($k = 10^8$ - 10^{10} mol s^{-1} L^{-1}) [41]. Therefore, the promotion of the reaction of •OH with organic compounds (instead of waste reactions) is strongly dependent on the concentration of organic matter in the solution.

$$\frac{d\,TOC(t)}{dt} = k_1 * TOC(t) \quad (9)$$

with k_1, the pseudo-first order rate constant

The use of a BDD electrode, as anode in the EF process, strongly increased the mineralization kinetics (k_1 = 0.12 and 0.38 h^{-1} for EF/Pt and EF/BDD, respectively) due to the higher contribution of heterogeneous •OH, generated on the surface of BDD anode, for mineralization of organic compounds, compared to Pt anode. Pt is an active anode and therefore it is not able of accumulating large amounts of •OH on its surface. The degradation of organic compounds take place can only from direct electron transfer, which is a selective mechanism contributing in a minor way to the mineralization. These results obtained in a real complex effluent confirm that a detailed mineralization kinetic model of EF-based processes should take into consideration both homogeneous reactions in the bulk and heterogeneous reaction at the anode, as proposed by Mousset et al. (2019) [42].

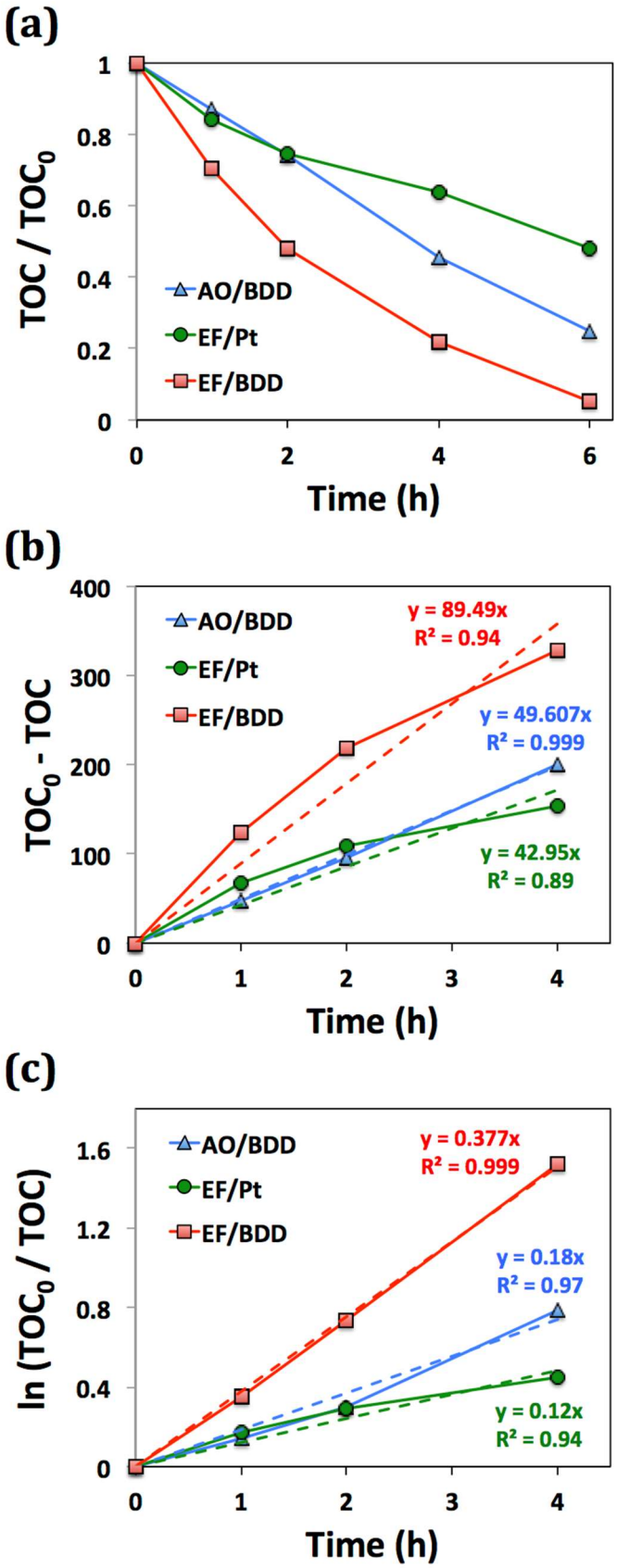
(a)
TOC / TOC0
Time (h)
AO/BDD
EF/Pt
EF/BDD
(b)
TOC0 - TOC
Time (h)
y = 89.49x
R² = 0.94
y = 49.607x
R² = 0.999
y = 42.95x
R² = 0.89
(c)
ln (TOC0 / TOC)
Time (h)
y = 0.377x
R² = 0.999
y = 0.18x
R² = 0.97
y = 0.12x
R² = 0.94

244

Figure 2 – Comparison of mineralization kinetics of the raw effluent by different processes at constant current intensity of 200 mA (8.3 mA cm^{-2}), including anodic oxidation with BDD anode (AO), electro-Fenton process with Pt anode (EF) and electro-Fenton with BDD anode (EF/BDD) (a). Linear regression analysis of mineralization kinetics following a pseudo-zero (b) and pseudo-first (c) order assumption.

3.3 Comparison of homogeneous (EF) and heterogeneous (AO) processes for degradation of dyes and evolution of by-products

The evolution of the UV-vis spectrum of the effluent during treatment by the different processes was then followed (Fig. 3). TOC is a parameter only assessing the mineralization yield of organic matter. However, the mineralization is a complex process generating several intermediates products during the degradation of organic compounds. Therefore, the formation of intermediates and end by-products is also an important phenomenon to be considered. The evolution of the shape of the UV-vis spectrum provided indications on the evolution of the nature of organic compounds in this complex effluent. As expected, the absorbance of the solution decreased during both processes because of the degradation of dyes. However, different behaviors were observed between EF and AO processes.

A very fast decrease of the absorbance was observed in the visible region (discoloration of the effluent) during the EF process (Fig. 3a). The color decreased rapidly owing to the fast reaction of $^{\bullet}OH$ generated homogeneously in the bulk with the aromatic structure of BDB previously identified as the main dye in the effluent. The absolute reaction rate constant of $^{\bullet}OH$ with dyes is usually in the range 10^9 - 10^{10} M^{-1} s^{-1} [43,44]. The absorbance in the UV region decreased much less rapidly because of the formation of degradation by-products absorbing in the UV region. For example, Fig. SI-3 shows the much slower decrease of the absorbance at 254 nm compared to 668 nm. The highest absorbance remains in the region of

271 the lowest wavelengths (220 – 240 nm), most probably due to the formation of short-chain
272 carboxylic acids (e.g., oxalic acid and formic acid, which have maximum absorbance in this
273 UV region). These final degradation by-products are slowly mineralized because of their
274 lower reaction rate constants with •OH (e.g., absolute reaction rate constant of 1.4×10^6 M^{-1}
275 s^{-1} for oxalic acid) [45,46].

276 A much slower discoloration of the effluent was observed during AO/BDD because of the
277 mass transport limitation of dye from the bulk to the electrode surface (Fig. 3c). The
278 discoloration kinetics (based on absorbance measured at λ_{max} = 668 nm) followed a pseudo-
279 first order kinetic with k_1 = 0.61 h^{-1} for AO and k_1 = 7.3 h^{-1} for EF/BDD processes. The
280 decrease of 75% of the absorbance at 668 nm required 2 h of treatment by AO/BDD
281 compared to only 0.17 h with EF/BDD. This is ascribed to much more favorable mass
282 transport conditions for reactions of dyes with •OH homogeneously formed in the bulk,
283 compared to reaction with •OH heterogeneously generated at the anode surface.

284 Besides, on the contrary to EF, the shape of the UV-vis spectrum of the effluent remained
285 similar during the whole treatment using AO/BDD process (Fig. 3b). For instance, the
286 decrease of the absorbance at 254 nm using AO/BDD process was close to the decrease
287 obtained at 668 nm (Fig. SI-3 and SI-4). These results indicate that the dye was rapidly
288 mineralized after its initial degradation step, without accumulation of aromatic by-products.
289 This phenomenon is tightly related to the specific way to generate •OH during AO with BDD
290 anode. In fact, a large amount of •OH is accumulated on the anode surface and direct electron
291 transfer can also occur for degradation of some by-products such as short-chain carboxylic
292 acids. Therefore, organic compounds can be rapidly mineralized once reached the anode
293 surface and only a low amount of by-products are able to diffuse from the anode surface to the
294 bulk solution. Mediated oxidation in the bulk, based on active chlorine or sulfate radical
295 species, could also have participated in oxidation mechanisms during AO/BDD [15,24,47].

296 However, the obtained results indicated that homogeneous oxidation of dyes in the bulk was
297 not very significant during AO/BDD. A complete combustion of organic compounds in the
298 vicinity of the anode surface seems to be the most consistent oxidation mechanism in this
299 case. It might be ascribed to (i) lower reaction rate of organic compounds with these oxidant
300 species and (ii) fast reaction of these oxidant species in the vicinity of the electrode surface
301 since the AO/BDD process was operated under current limitation.

302 Overall, both processes present advantages and drawbacks. Homogeneous oxidation in the
303 bulk during EF with Pt anode allowed for fast degradation of dyes but further intermediates
304 might be accumulated in the solution. Heterogeneous oxidation at the anode surface during
305 AO allowed for complete mineralization of organic compounds with low accumulation of
306 intermediates but slower degradation kinetic of dyes. Therefore, combining EF with a non-
307 active electrode such as BDD appears as an appropriate solution to take advantage of both
308 ways to generate simultaneously homogeneous/heterogeneous $^{\bullet}OH$ for a quick removal of
309 organic compounds.

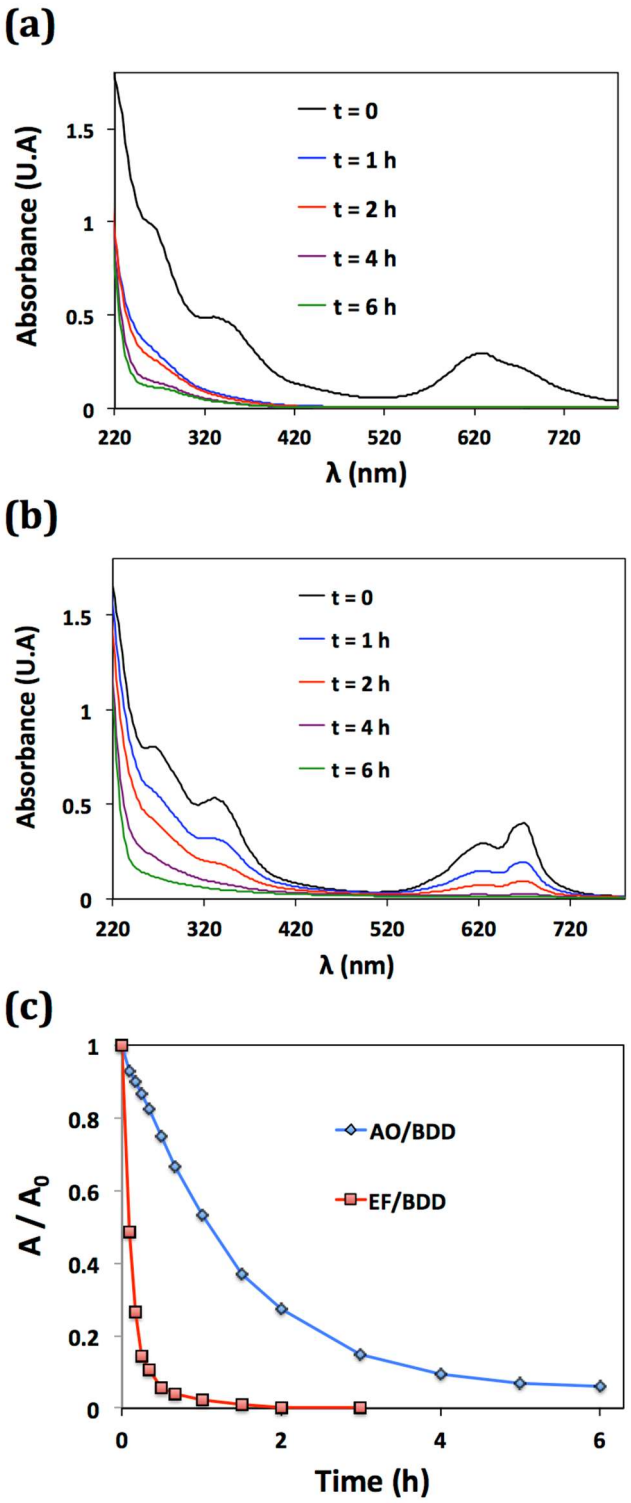

Figure 3 – Evolution of the UV-vis spectrum of the effluent during treatment by electro-Fenton process with BDD anode (EF/BDD) (a) and anodic oxidation with BDD anode (AO/BDD) (b). The slight difference of the spectrum at t = 0 was ascribed to the different pH of the effluent (i.e. natural pH for AO/BDD and pH 3 for EF/Pt). Figure (c) represents the comparison of the evolution of the absorbance at λ_{max} = 668

316 nm during EF/BDD and AO/BDD. This parameter corresponds to the discoloration of
317 the effluent.

318

319 **3.4 Influence of the current on AO/BDD and EF/BDD process efficiency**

320 The effectiveness for degradation and mineralization of AO/BDD and EF/BDD processes was
321 then compared at 200 mA (8.3 mA cm^{-2}) and 500 mA (21 mA cm^{-2}) (Fig. 4). For AO/BDD,
322 increasing the current supply strongly improved both discoloration of the effluent (i.e.,
323 degradation of the dye) and mineralization rate of organic compounds (Fig. 4a and 4b). As the
324 process was initially operated under current limitation conditions, increasing the generation of
325 $^{\bullet}OH$ strongly increased the effectiveness of the process during the first two hours of treatment.
326 However, the limiting current density was then reached as soon as the TOC removal rate
327 reached around 40-50% for I = 500 mA (according to Eq. 7). Therefore, the evolution of TOC
328 did not follow a pseudo-zero order kinetic since the process was then operated under mass
329 transport control. The decrease of organic matter in the solution reduced the transport rate
330 towards the anode and promoted dimerization of $^{\bullet}OH$ (Eq. 10). Therefore, the mineralization
331 rate decreased compared to that observed during the first 2 hours of treatment performed
332 under current limitation.

333 $$2\ BDD(^{\bullet}OH) \rightarrow 2\ BDD + H_2O_2 \qquad (10)$$

334 As regards to the EF/BDD process, higher current intensity increased reaction rates of O_2 and
335 Fe^{3+} reduction, as well as $^{\bullet}OH$ formation at the anode. A beneficial effect was therefore
336 observed on both discoloration of the effluent and mineralization of organic matter (Fig. 4c
337 and 4d). However, the increase of the concentration of H_2O_2, Fe^{2+} and consequently of $^{\bullet}OH$ in
338 the bulk can also promote several parasitic reactions (Eq. 11 – 13).

339 $$Fe^{2+} + {}^{\bullet}OH \rightarrow Fe^{3+} + OH^{-} \qquad (11)$$

340 $H_2O_2 + {}^{\bullet}OH \rightarrow H_2O + HO_2^{\bullet}$ (12)

341 $HO_2^{\bullet} + {}^{\bullet}OH \rightarrow H_2O + O_2$ (13)

342 Overall, increasing the current accelerates discoloration kinetics and mineralization rates in all
343 cases. However, it also has strong adverse effects on the energy efficiency of the process
344 because of the promotion of (i) mass transport limitations for heterogeneous reaction at the
345 anode and (ii) parasitic reactions of $^{\bullet}OH$ generated in the bulk during EF process. This fact
346 can be highlighted by the calculation of the energy consumption (EC) of the process, which
347 strongly increases at high currents in both cases (Fig. 5). This figure shows that EC (expressed
348 as kWh $(kgTOC)^{-1}$) can be maintained almost constant when operating AO under conditions
349 of current limitation (experiment at 200 mA), since the mineralization rate remains constant.
350 Under mass transport limitation (i.e., at higher current densities), EC increases with time
351 during AO because of the increase of wasting reaction (Eq. 10) when the amount of organic
352 matter becomes low (Fig. 5a). The increase of the current intensity also has an adverse effect
353 on cell potential (5.2 and 7.3 V at 200 and 500 mA, respectively), which has a direct impact
354 on EC according to the Eq. 6.

355 As highlighted by the Fig. 5b, the EF/BDD process allows for decreasing EC thanks to the
356 faster mineralization rate ascribed to the formation of oxidant species both at the anode and in
357 the bulk. For example, after 4 h of treatment, the EC was 90 and 55 kWh $(kgTOC)^{-1}$ for
358 AO/BDD and EF/BDD processes, respectively. However, the EC was more affected by the
359 treatment time in EF than in AO under current limitation since the oxidation rate in the bulk is
360 a phenomenon depending on the concentration of organic compounds.

361 At 200 mA, the treatment during 4 h by the EF/BDD process resulted in 78% TOC removal
362 with an EC value of 18 kWh m^{-3}. This value of EC is in the low range of values reported by
363 Brillas and Martinez-Huítle (2015) [7] while most of values reported in this review

correspond to experiments performed on synthetic effluents containing dyes at concentration in the range 100 – 500 mg L^{-1}. This comparison highlights that the use of BDD anode in EF process constitutes an efficient approach to remove organic pollutants in a non-selective way.

Similar conclusions were obtained from calculation of the current efficiency based on COD removal (CE_{COD}). The CE_{COD} calculated after 4 h of treatment by AO/BDD at 200 mA and 500 mA was 51% and 25%, respectively. The decrease of CE_{COD} at high current intensity directly highlights the increase of wasting reaction (Eq. 10). By comparison, the CE_{COD} after 4 h of treatment by EF/BDD at 200 mA was 78%. This higher value compared to the AO/BDD process highlights the benefit of the formation of oxidants in the bulk from the electrochemically generated Fenton's reagent.

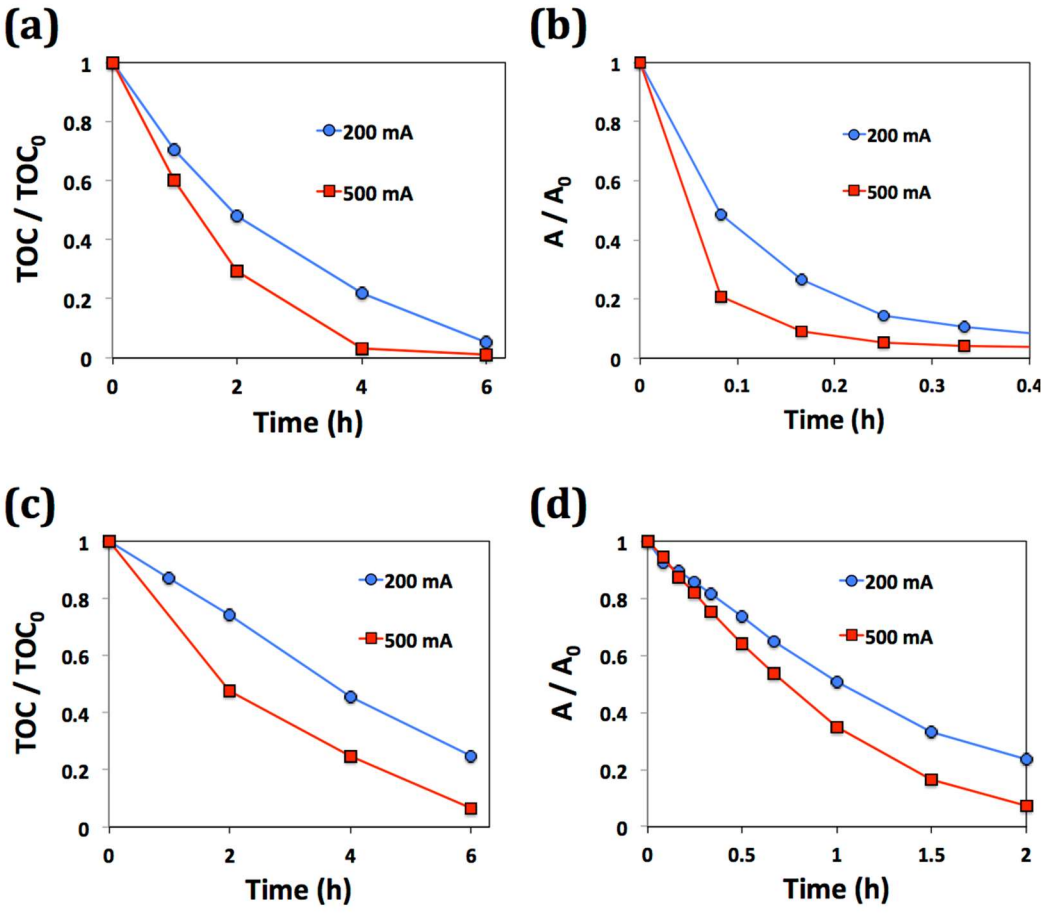

Figure 4 – Comparison of mineralization (a, c) and discoloration (at λ_{max} = 668 nm) (b, d) kinetics during the treatment by anodic oxidation with BDD anode (c, d) and electro-Fenton with BDD anode (a, b) at 200 and 500 mA.

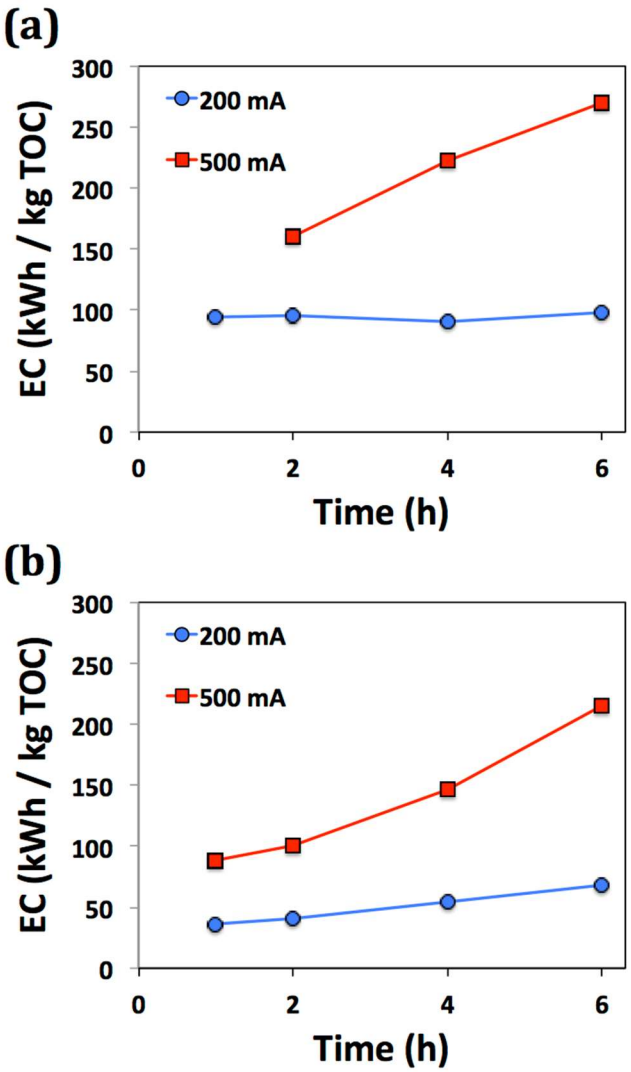

Figure 5 – Evolution with time of the energy consumption for the treatment of the industrial effluent by anodic oxidation with BDD anode (a) and electro-Fenton with BDD anode (b) at I = 200 and 500 mA.

3.5 Influence of initial pH of the effluent on AO process

The EF/BDD process requires operating at an optimal pH of 3 in order to maintain the concentration of the catalyst Fe^{2+} in the solution. Inversely, the AO process can operate in a

wider pH range since •OH are generated from oxidation of H_2O. Therefore, the results presented in Fig. 6 aimed at studying the effect of initial pH of the effluent on the effectiveness of the AO process. There was not any significant difference in the mineralization effectiveness obtained at pH 3, 8 and 13.4 (natural pH of the effluent) (Fig. 6). Protonation / deprotonation of organics in the solution did not significantly impact the overall mineralization yield. This behavior would also be a key advantage in case of pH fluctuation of the effluent to treat.

As the initial pH of the solution was 13.4, pH adjustment would represent an important cost for the EF/BDD process that may strongly counterbalance the lower EC. The AO process would clearly have the advantage to avoid this pH adjustment step. It is why recent researches are currently focusing on the development of heterogeneous catalysts for implementation of EF-like processes in a wider range of pH [48–50].

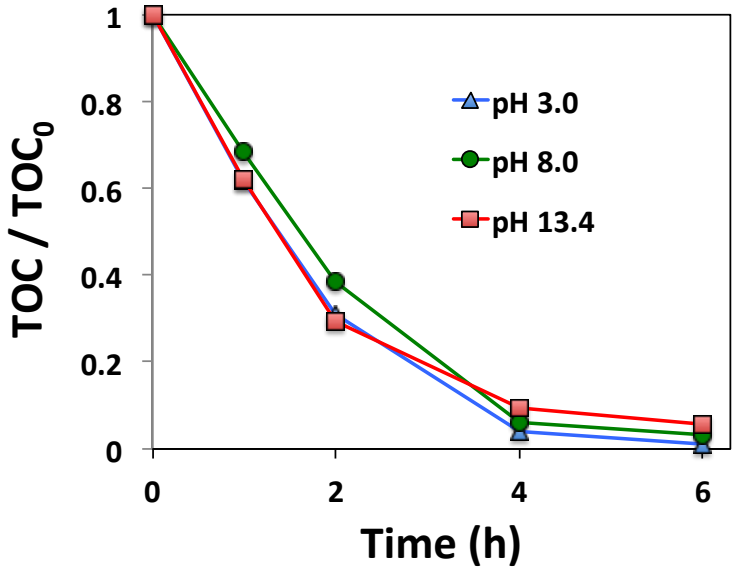

Figure 6 – Comparison of mineralization kinetics of the effluent at different initial pH (3, 8 and 13.4, i.e., the natural pH of the effluent) during the treatment by anodic oxidation (AO) with BDD anode at 500 mA.

3.6 Formation of chlorate and perchlorate at BDD anode

One of the most important drawbacks of EAOPs is the formation of ClO_3^- and ClO_4^- from Cl^- evolution at the surface of anode materials (Eq. 14). Particularly, the conversion of ClO_3^- and ClO_4^- occurs is promoted at the surface of BDD anode because it is able to catalyze both direct electron transfer and $^{\bullet}OH$ mediated oxidation, as detailed in Eq. 15 and 16 [35,51].

$$Cl^- \rightarrow ClO^- \rightarrow ClO_2^- \rightarrow ClO_3^- \rightarrow ClO_4^- \quad (14)$$

$$ClO_3^- \rightarrow ClO_3^{\bullet} + e^- \quad (15)$$

$$ClO_3^{\bullet} + OH^{\bullet} \rightarrow HClO_4 \quad (16)$$

The results presented in Fig. 7 shows the evolution of the concentration of ClO_3^- and ClO_4^- during the treatment by AO/BDD and EF/Pt at different current intensities. Fig. 8 shows the evolution of the CE for oxidation of Cl^- to ClO_3^- and ClO_4^- (CE_{ClOx}). On the contrary to CE for COD removal, increasing the current intensity did not reduce CE_{ClOx}. These results are consistent with the study of Zöllig et al. (2015) on the treatment of urine with BDD anode [52]. Therefore, a very fast conversion of Cl^- to ClO_3^- was initially observed at 500 and 1000 mA. Then the concentration of ClO_3^- decreased because of its further conversion to ClO_4^-. ClO_3^- behaved as an intermediate compound with an evolution of its concentration depending both on (i) its formation rate from Cl^- and (ii) its destruction rate with formation of stable ClO_4^-. Thus, the concentration of ClO_3^- started to decrease in the bulk when its destruction rate was higher than the formation rate. It occurred along the treatment due to the strong decrease with time of the concentration of Cl^- reducing its formation rate. For example, 89% of the initial concentration of Cl^- was oxidized/transformed after 6 h of treatment at 1000 mA. However, the CE for Cl^- oxidation to both ClO_3^- and ClO_4^- did not significantly decrease over

time during treatment by AO/BDD at 200 and 500 mA, which is also consistent with the previous study on the treatment of urine with BDD anode [52]. A decrease was only observed at the highest current of 1000 mA, for which the concentration of Cl^- reached the lowest values.

It is interesting to notice that the formation of ClO_4^- started from the very beginning of the treatment by AO/BDD. By comparison, Pérez et al. (2012) previously described the evolution of chlorinated species at BDD anode in synthetic solution containing Cl^- and NH_4^+ as well as in real landfill leachates [53]. In this case, the formation of ClO_4^- in the synthetic solution only appeared after 2 hours of treatment at 40 mA cm^{-2}. Similar delay for formation of ClO_4^- was reported during treatment of urine [52]. The rapid formation of ClO_4^- without any delay in the case of this textile effluent under study was most probably related to different conditions for competitive reactions, such as the absence of $N\text{-}NH_4^+$ and the different nature of organic compounds. For example, high concentrations of NH_4^+ in landfill leachates and urine initially involves competitive reactions of active chlorine with NH_4^+ for formation of mono-, di-, tri-chloramines, N_2 or NO_3^- [53]. Donaghue et al. (2013) also highlighted that perchlorate formation might be inhibited from $^{\bullet}OH$ scavenging by organic compounds, owing to the reduction of the availability of $^{\bullet}OH$ for reaction with $ClO_3^{\bullet}$ in the vicinity of the electrode (Eq. 16) [35]. Such inhibition phenomenon was clearly depending on the reactivity of the organic compound selected as $^{\bullet}OH$ scavenger.

The formation rate of ClO_4^- at different current intensities can be compared during the first hour of treatment (during which the concentration of Cl^- remains comparable for all experiments). Compared to the experiment at 200 mA, the concentration of ClO_4^- formed at 500 and 1000 mA was multiplied by 3.1 and 8.3, respectively. These values are higher than the increase of the electric charge consumed, which was multiplied by 2.5 and 5 at 500 and 1000 mA, respectively. These results indicate that using low current intensity slightly reduced

the formation of ClO_4^-. It might be explained by the operation of the process under current limitation at 200 mA, which favors total $^{\bullet}OH$ scavenging by reaction with organic compounds [35]. However, an additional test showed that further decreasing the current intensity to 50 mA (2.1 mA cm^{-2}) did not further reduced the formation of perchlorate compared to the experiment performed at 200 mA for a similar electrical charge. By comparison to the study of Donaghue et al. (2013) [35], much lower inhibition of ClO_4^- formation was therefore observed in this study. The difference might be ascribed to the different pH conditions (4.4 *vs* 13.4), which was previously reported as an important factor for these reactions [52,54,55], as well as by the different nature of organic compounds. These results highlight that the formation of ClO_3^- and ClO_4^- should always be monitored carefully during the application of heterogeneous EAOPs using non-active anode materials. They also emphasize the need to continue further research on ClO_4^- formation and competition phenomena at the surface of these anodes.

The formation of ClO_3^- and ClO_4^- during the AO/BDD process was then compared with the EF/Pt process. It is interesting to notice that the formation of ClO_4^- remained below the detection limit during the treatment of this effluent by EF/Pt process (Fig. 7). This configuration presents the crucial advantage of using an active anode material (Pt) that reduces the formation of ClO_4^- because of the low accumulation of $^{\bullet}OH$ at the surface [51]. For example, the formation of ClO_4^- was around 50 times lower when using Pt instead of BDD anode during treatment at 20 mA cm^{-2} of drinking water containing 230 mg L^{-1} of Cl^- [51]. The formation of ClO_3^- was also strongly reduced in the configuration EF-Pt. Very low concentration of ClO_3^- was obtained all along the treatment at 200 mA (below 0.5% of the initial Cl^- concentration). Compared to BDD, the absence of oxidation of Cl^- by $^{\bullet}OH$ at the anode surface might reduce the formation rate. Moreover, a previous study from Jung et al. (2010) highlighted that formation (and accumulation) of active chlorine was a key

intermediate step for increasing ClO_3^- formation rate at Pt anode [55]. Therefore, competitive reaction of active chlorine with organic compounds might also have reduced the formation of ClO_3^-. The lower pH required for EF experiments (pH 3) also participated to reduce the formation of ClO_3^-. In fact, alkaline pH was reported to be more favorable since HOCl participate in a lower extent to the formation of ClO_3^- than OCl^- [55]. Higher formation rate was obtained at 1000 mA since the chlorine demand might have been reached more rapidly at high current intensity (because of further formation of active chlorine). For example, ClO_3^- appeared only after 2 h of treatment, most probably because of the preferential reaction of active chlorine with organic compounds at the beginning of the treatment. Once the chlorine demand is reached, active chlorine can accumulate in the solution and further reaction to ClO_3^- can occur more easily. However, the CE_{ClOx} for Cl^- oxidation was still much lower compared to the AO/BDD configuration at the same current intensity (Fig. 8). Therefore, using an anode material and operating conditions that prevent the formation of ClO_3^- / ClO_4^- would be crucial for application of the EF process. Dimensionally stable anodes (RuO_2/IrO_2) might be a suitable low-cost alternative since it is an active material avoiding the accumulation of hydroxyl radicals at its surface [51].

Reaction of active chlorine with organic compounds might also lead to the formation of organochlorinated by products, which are usually considered as toxic compounds. Stripping of the most volatile compounds might occur [52]. However, using an analytical tool such as the measurement of adsorbable organic halides (AOX) would be interesting for monitoring the fate (formation/degradation) of these compounds during the treatment. This issue should also be taken into consideration for optimization of process operation and assessment of the suitability of EAOPs for treatment of chloride-containing water.

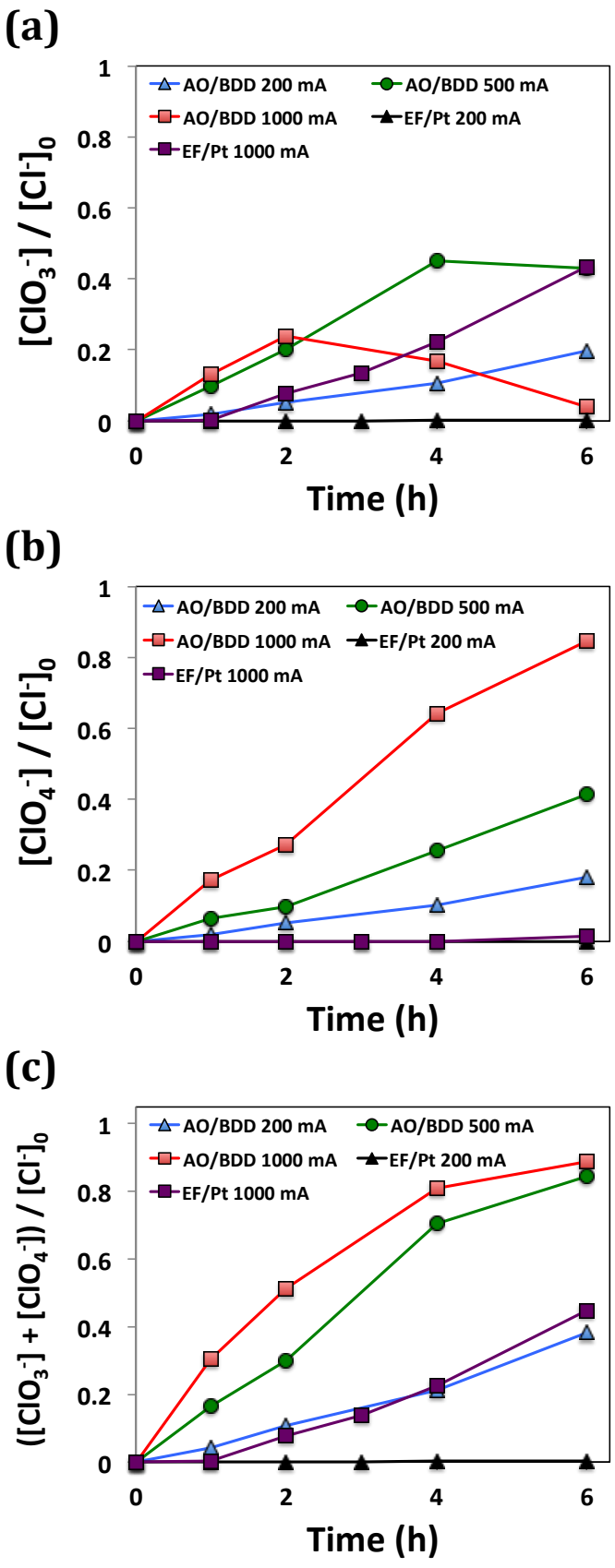

501

502 **Figure 7 –** Evolution of the concentration of ClO_3^- (a) and ClO_4^- (b) and sum of both
503 (c) during the treatment of the real effluent by anodic oxidation process (natural pH of

13.4) with BDD anode at (-▲-) 200 mA (8.3 mA cm^{-2}), (-●-) 500 mA (21 mA cm^{-2}) and (-■-) 1000 mA (42 mA cm^{-2}) and electro-Fenton process (pH 3) with Pt anode at (-▲-) 200 mA and (-■-) 1000 mA. All molar concentrations were normalized as regards to the initial concentration of Cl^- in the effluent.

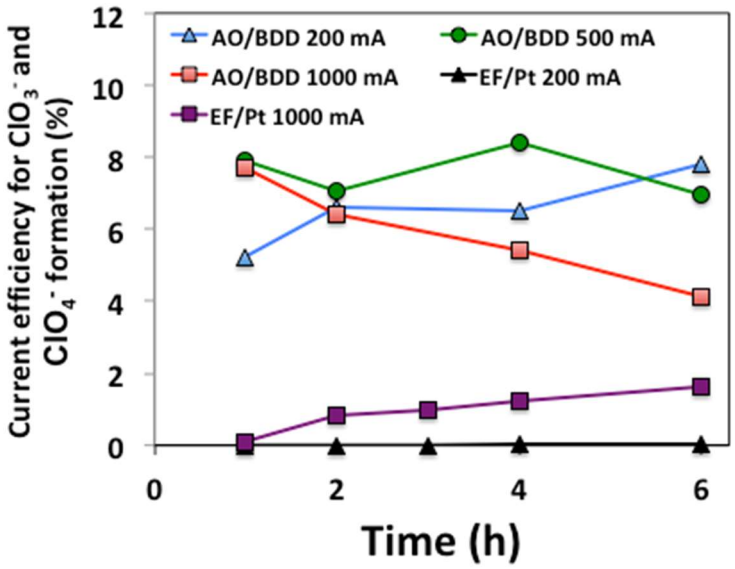

Figure 8 – Current efficiency for ClO_3^- and ClO_4^- formation from Cl^- oxidation during the treatment by anodic oxidation process with BDD anode (natural pH of 13.4) at (-▲-) 200 mA (8.3 mA cm^{-2}), (-●-) 500 mA (21 mA cm^{-2}) and (-■-) 1000 mA (42 mA cm^{-2}) and electro-Fenton process with Pt anode at 200 (-▲-) 200 mA and (-■-) 1000 mA.

4. Conclusions

This study allowed for understanding the impact of the generation of oxidant species homogeneously in the bulk (EF) or heterogeneously at the surface of BDD electrode (AO) during the treatment of a real effluent coming from the textile industry. Both EAOPs achieved non-selective mineralization of organic compounds in the effluent. However, different behaviors were highlighted.

- Faster discoloration (i.e. degradation of dyes) kinetics was obtained by EF compared to AO thanks to more favorable mass transport conditions for reaction of dyes with $^{\bullet}OH$ homogeneously generated in the bulk.
- Lower accumulation of by-products was obtained during AO because of complete combustion of dyes in the vicinity of the anode surface where high concentration of $^{\bullet}OH$ is accumulated.
- The mineralization rate was constant with time for AO operated under current limitation condition (pseudo-zero order kinetic) while it decreased with time (pseudo-first order kinetic) for EF/Pt and EF/BDD processes.
- A lower EC and higher CE were achieved for EF/BDD compared to AO thanks to generation of oxidant species from both anodic and cathodic processes. EC increases with treatment time when mass transport limitations occur.
- Mineralization effectiveness remained constant during AO regardless of the initial pH of the effluent.
- Using non-active anode material such as BDD involves the formation of large amounts of ClO_3^- and ClO_4^-; the inhibition of perchlorate formation under current limitation was lower than the one expected from studies on synthetic solutions.
- Implementation of the EF process with active electrode (Pt) allowed for a strong decrease of the formation of ClO_3^- and ClO_4^-; the conversion even remained below 0.5% of the initial Cl^- concentration when using low current intensity.

An important challenge is to control the evolution of chlorinated inorganic species, while achieving efficient removal of the organic load. These results highlight that future studies could focus on (i) the development of electrode materials with low reactivity for conversion of Cl^- to ClO_3^- and ClO_4^-, (ii) the development of heterogeneous EF-like processes with active

anodes that could be implemented in a wider pH range, and (iii) the combination of EAOPs with a post-treatment for the removal of these chlorinated inorganic compounds.

Acknowledgments

This work is dedicated to the memory of the late Professor Adouby Kopoin of INP-HB (scientific supervisor) who unfortunately passed away in January 2021. Authors are grateful to the Service de Coopération et d'Action Culturelle (SCAC) of the French Embassy for providing financial support for the mobility of Alain Sié HIEN at Laboratoire Géomatériaux et Environnement. This work is part of the Public-Private Partnership Project funded by the Programme d'Appui Stratégique à la Recherche Scientifique (PASRES) and the African Centre for Technology Studies (ACTS)

.

References

[1] A.S. Assémian, K.E. Kouassi, A.E. Zogbé, K. Adouby, P. Drogui, In-situ generation of effective coagulant to treat textile bio-refractory wastewater: Optimization through response surface methodology, Journal of Environmental Chemical Engineering. 6 (2018) 5587–5594. https://doi.org/10.1016/j.jece.2018.08.050.

[2] F. Mekhalef Benhafsa, S. Kacha, A. Leboukh, K.D. Belaid, Étude comparative de l'adsorption du colorant Victoria Bleu Basique à partir de solutions aqueuses sur du carton usagé et de la sciure de bois, Revue des sciences de l'eau. 31 (2018) 109–126. https://doi.org/10.7202/1051695ar.

[3] E. Pajootan, M. Arami, N.M. Mahmoodi, Binary system dye removal by electrocoagulation from synthetic and real colored wastewaters, Journal of the Taiwan Institute of Chemical Engineers. 43 (2012) 282–290. https://doi.org/10.1016/j.jtice.2011.10.014.

[4] H. Mansour, O. Boughzala, D. Dridi, D. Barillier, L. Chekir-Ghedira, R. Mosrati, Les colorants textiles sources de contamination de l'eau : CRIBLAGE de la toxicité et des méthodes de traitement, rseau. 24 (2011) 209–238. https://doi.org/10.7202/1006453ar.

[5] P. Aravind, H. Selvaraj, S. Ferro, M. Sundaram, An integrated (electro- and bio-oxidation) approach for remediation of industrial wastewater containing azo-dyes: Understanding the degradation mechanism and toxicity assessment, Journal of Hazardous Materials. 318 (2016) 203–215. https://doi.org/10.1016/j.jhazmat.2016.07.028.

[6] L. Gebrati, M. El Achaby, H. Chatoui, M. Laqbaqbi, J. El Kharraz, F. Aziz, Inhibiting effect of textile wastewater on the activity of sludge from the biological treatment process of the activated sludge plant, Saudi Journal of Biological Sciences. 26 (2019) 1753–1757. https://doi.org/10.1016/j.sjbs.2018.06.003.

[7] E. Brillas, C.A. Martínez-Huitle, Decontamination of wastewaters containing synthetic organic dyes by electrochemical methods. An updated review, Applied Catalysis B: Environmental. 166–167 (2015) 603–643. https://doi.org/10.1016/j.apcatb.2014.11.016.

[8] V. Khandegar, A.K. Saroha, Electrocoagulation for the treatment of textile industry effluent – A review, Journal of Environmental Management. 128 (2013) 949–963. https://doi.org/10.1016/j.jenvman.2013.06.043.

[9] T. Mandal, D. Dasgupta, S. Mandal, S. Datta, Treatment of leather industry wastewater by aerobic biological and Fenton oxidation process, Journal of Hazardous Materials. 180 (2010) 204–211. https://doi.org/10.1016/j.jhazmat.2010.04.014.

[10] M. Constapel, M. Schellenträger, J.M. Marzinkowski, S. Gäb, Degradation of reactive dyes in wastewater from the textile industry by ozone: Analysis of the products by accurate masses, Water Research. 43 (2009) 733–743. https://doi.org/10.1016/j.watres.2008.11.006.

[11] G. Ciardelli, N. Ranieri, The treatment and reuse of wastewater in the textile industry by means of ozonation and electroflocculation, Water Research. 35 (2001) 567–572. https://doi.org/10.1016/S0043-1354(00)00286-4.

[12] A.L. Barros, T.M. Pizzolato, E. Carissimi, I.A.H. Schneider, Decolorizing dye wastewater from the agate industry with Fenton oxidation process, Minerals Engineering. 19 (2006) 87–90. https://doi.org/10.1016/j.mineng.2005.04.004.

[13] T. Ölmez, I. Kabdaşlı, O. Tünay, The effect of the textile industry dye bath additive EDTMPA on colour removal characteristics by ozone oxidation, Water Science and Technology. 55 (2007) 145–153. https://doi.org/10.2166/wst.2007.317.

[14] P. Bautista, A.F. Mohedano, J.A. Casas, J.A. Zazo, J.J. Rodriguez, An overview of the application of Fenton oxidation to industrial wastewaters treatment, J. Chem. Technol. Biotechnol. 83 (2008) 1323–1338. https://doi.org/10.1002/jctb.1988.

[15] C.A. Martínez-Huitle, M.A. Rodrigo, I. Sirés, O. Scialdone, Single and Coupled Electrochemical Processes and Reactors for the Abatement of Organic Water Pollutants: A Critical Review, Chem. Rev. 115 (2015) 13362–13407. https://doi.org/10.1021/acs.chemrev.5b00361.

[16] I. Sirés, E. Brillas, M.A. Oturan, M.A. Rodrigo, M. Panizza, Electrochemical advanced oxidation processes: today and tomorrow. A review, Environmental Science and Pollution Research. 21 (2014) 8336–8367. https://doi.org/10.1007/s11356-014-2783-1.

[17] M.A. Oturan, Electrochemical advanced oxidation technologies for removal of organic pollutants from water, Environ Sci Pollut Res. 21 (2014) 8333–8335. https://doi.org/10.1007/s11356-014-2841-8.

[18] M.A. Oturan, Outstanding performances of the BDD film anode in electro-Fenton process: Applications and comparative performance, Current Opinion in Solid State and Materials Science. 25 (2021) 100925. https://doi.org/10.1016/j.cossms.2021.100925.

[19] Á. Anglada, A.M. Urtiaga, I. Ortiz, Laboratory and pilot plant scale study on the electrochemical oxidation of landfill leachate, Journal of Hazardous Materials. 181 (2010) 729–735. https://doi.org/10.1016/j.jhazmat.2010.05.073.

[20] B.P. Chaplin, Critical review of electrochemical advanced oxidation processes for water treatment applications, Environ. Sci.: Processes Impacts. (2014). https://doi.org/10.1039/C3EM00679D.

[21] O. Ganzenko, C. Trellu, N. Oturan, D. Huguenot, Y. Péchaud, E.D. van Hullebusch, M.A. Oturan, Electro-Fenton treatment of a complex pharmaceutical mixture: Mineralization efficiency and biodegradability enhancement, Chemosphere. 253 (2020) 126659. https://doi.org/10.1016/j.chemosphere.2020.126659.

[22] C. Trellu, Y. Péchaud, N. Oturan, E. Mousset, D. Huguenot, E.D. van Hullebusch, G. Esposito, M.A. Oturan, Comparative study on the removal of humic acids from drinking water by anodic oxidation and electro-Fenton processes: Mineralization efficiency and modelling, Applied Catalysis B: Environmental. 194 (2016) 32–41. https://doi.org/10.1016/j.apcatb.2016.04.039.

[23] W.M. Latimer, Oxidation Potentials, Prentice-Hall, 1952.

[24] M. Panizza, G. Cerisola, Direct and mediated anodic oxidation of organic pollutants, Chem. Rev. 109 (2009) 6541–6569. https://doi.org/10.1021/cr9001319.

[25] A. Kapałka, G. Fóti, C. Comninellis, The importance of electrode material in environmental electrochemistry: Formation and reactivity of free hydroxyl radicals on boron-doped diamond electrodes, Electrochimica Acta. 54 (2009) 2018–2023. https://doi.org/10.1016/j.electacta.2008.06.045.

[26] E. Brillas, I. Sirés, M.A. Oturan, Electro-Fenton process and related electrochemical technologies based on Fenton's reaction chemistry, Chemical Reviews. 109 (2009) 6570–6631. https://doi.org/10.1021/cr900136g.

[27] M. Zhou, M.A. Oturan, I. Sirés, eds., Electro-Fenton Process: New Trends and Scale-Up, Springer Singapore, 2018. https://doi.org/10.1007/978-981-10-6406-7.

[28] N. Oturan, J. Bo, C. Trellu, M.A. Oturan, Comparative Performance of Ten Electrodes in Electro-Fenton Process for Removal of Organic Pollutants from Water, ChemElectroChem. 8 (2021) 3294–3303. https://doi.org/10.1002/celc.202100588.

[29] S. Raghu, C.W. Lee, S. Chellammal, S. Palanichamy, C.A. Basha, Evaluation of electrochemical oxidation techniques for degradation of dye effluents—A comparative approach, Journal of Hazardous Materials. 171 (2009) 748–754. https://doi.org/10.1016/j.jhazmat.2009.06.063.

[30] C. Espinoza, J. Romero, L. Villegas, L. Cornejo-Ponce, R. Salazar, Mineralization of the textile dye acid yellow 42 by solar photoelectro-Fenton in a lab-pilot plant, Journal of Hazardous Materials. 319 (2016) 24–33. https://doi.org/10.1016/j.jhazmat.2016.03.003.

[31] F.E. Titchou, H. Zazou, H. Afanga, E.G. Jamila, R. Ait Akbour, M. Hamdani, M.A. Oturan, Comparative study of the removal of direct red 23 by anodic oxidation, electro-Fenton, photo-anodic oxidation and photoelectro-Fenton in chloride and sulfate media, Environ Res. 204 (2022) 112353. https://doi.org/10.1016/j.envres.2021.112353.

[32] P.V. Nidheesh, M. Zhou, M.A. Oturan, An overview on the removal of synthetic dyes from water by electrochemical advanced oxidation processes, Chemosphere. 197 (2018) 210–227. https://doi.org/10.1016/j.chemosphere.2017.12.195.

[33] A.V. Karim, P.V. Nidheesh, M.A. Oturan, Boron-doped diamond electrodes for the mineralization of organic pollutants in the real wastewater, Current Opinion in Electrochemistry. 30 (2021) 100855. https://doi.org/10.1016/j.coelec.2021.100855.

[34] J. Radjenovic, D.L. Sedlak, Challenges and Opportunities for Electrochemical Processes as Next-Generation Technologies for the Treatment of Contaminated Water, Environ. Sci. Technol. 49 (2015) 11292–11302. https://doi.org/10.1021/acs.est.5b02414.

[35] A. Donaghue, B.P. Chaplin, Effect of Select Organic Compounds on Perchlorate Formation at Boron-doped Diamond Film Anodes, Environ. Sci. Technol. 47 (2013) 12391–12399. https://doi.org/10.1021/es4031672.

[36] C. Trellu, N. Oturan, F.K. Keita, C. Fourdrin, Y. Pechaud, M.A. Oturan, Regeneration of Activated Carbon Fiber by the Electro-Fenton Process, Environ. Sci. Technol. 52 (2018) 7450–7457. https://doi.org/10.1021/acs.est.8b01554.

[37] I. Belbachir, B. Makhoukhi, Adsorption of Bezathren dyes onto sodic bentonite from aqueous solutions, Journal of the Taiwan Institute of Chemical Engineers. 75 (2017) 105–111.

https://doi.org/10.1016/j.jtice.2016.09.042.

[38] Ministère de l'environnement et de la forêt, République de Côte d'Ivoire, Arrêté N° 01164 du 04/11/2008, n.d.

[39] W.H. Organization, WHO Guidelines for the Safe Use of Wasterwater Excreta and Greywater, World Health Organization, 2006.

[40] M.A. Rodrigo, P.A. Michaud, I. Duo, M. Panizza, G. Cerisola, C. Comninellis, Oxidation of 4-chlorophenol at boron-doped diamond electrode for wastewater treatment, J. Electrochem. Soc. 148 (2001) D60–D64. https://doi.org/10.1149/1.1362545.

[41] G. Buxton, C. Greenstock, W. Helman, A. Ross, Critical-Review of Rate Constants for Reactions of Hydrated Electrons, Hydrogen-Atoms and Hydroxyl Radicals (.oh/.o-) in Aqueous-Solution, J. Phys. Chem. Ref. Data. 17 (1988) 513–886.

[42] E. Mousset, Y. Pechaud, N. Oturan, M.A. Oturan, Charge transfer/mass transport competition in advanced hybrid electrocatalytic wastewater treatment: Development of a new current efficiency relation, Applied Catalysis B: Environmental. 240 (2019) 102–111. https://doi.org/10.1016/j.apcatb.2018.08.055.

[43] A. Ozcan, M.A. Oturan, N. Oturan, Y. Sahin, Removal of Acid Orange 7 from water by electrochemically generated Fenton's reagent, J Hazard Mater. 163 (2009) 1213–1220. https://doi.org/10.1016/j.jhazmat.2008.07.088.

[44] A. Lahkimi, M.A. Oturan, N. Oturan, M. Chaouch, Removal of textile dyes from water by the electro-Fenton process, Environ Chem Lett. 5 (2007) 35–39. https://doi.org/10.1007/s10311-006-0058-x.

[45] Knud. Sehested, Nikola. Getoff, F. Schwoerer, V.M. Markovic, S.O. Nielsen, Pulse radiolysis of oxalic acid and oxalates, J. Phys. Chem. 75 (1971) 749–755. https://doi.org/10.1021/j100676a004.

[46] M.A. Oturan, M. Pimentel, N. Oturan, I. Sirés, Reaction sequence for the mineralization of the short-chain carboxylic acids usually formed upon cleavage of aromatics during electrochemical Fenton treatment, Electrochimica Acta. 54 (2008) 173–182. https://doi.org/10.1016/j.electacta.2008.08.012.

[47] A. Farhat, J. Keller, S. Tait, J. Radjenovic, Oxidative capacitance of sulfate-based boron-doped diamond electrochemical system, Electrochemistry Communications. 89 (2018) 14–18. https://doi.org/10.1016/j.elecom.2018.02.007.

[48] S.O. Ganiyu, M. Zhou, C.A. Martínez-Huitle, Heterogeneous electro-Fenton and photoelectro-Fenton processes: A critical review of fundamental principles and application for water/wastewater treatment, Applied Catalysis B: Environmental. 235 (2018) 103–129. https://doi.org/10.1016/j.apcatb.2018.04.044.

[49] N. Barhoumi, H. Olvera-Vargas, N. Oturan, D. Huguenot, A. Gadri, S. Ammar, E. Brillas, M.A. Oturan, Kinetics of oxidative degradation/mineralization pathways of the antibiotic tetracycline by the novel heterogeneous electro-Fenton process with solid catalyst chalcopyrite, Applied Catalysis B: Environmental. 209 (2017) 637–647. https://doi.org/10.1016/j.apcatb.2017.03.034.

[50] L. Labiadh, M.A. Oturan, M. Panizza, N.B. Hamadi, S. Ammar, Complete removal of AHPS synthetic dye from water using new electro-fenton oxidation catalyzed by natural pyrite as heterogeneous catalyst, Journal of Hazardous Materials. 297 (2015) 34–41. https://doi.org/10.1016/j.jhazmat.2015.04.062.

[51] M.E.H. Bergmann, J. Rollin, T. Iourtchouk, The occurrence of perchlorate during drinking water electrolysis using BDD anodes, Electrochimica Acta. 54 (2009) 2102–2107. https://doi.org/10.1016/j.electacta.2008.09.040.

[52] H. Zöllig, A. Remmele, C. Fritzsche, E. Morgenroth, K.M. Udert, Formation of Chlorination Byproducts and Their Emission Pathways in Chlorine Mediated Electro-Oxidation of Urine on Active and Nonactive Type Anodes, Environ. Sci. Technol. 49 (2015) 11062–11069. https://doi.org/10.1021/acs.est.5b01675.

[53] G. Pérez, J. Saiz, R. Ibañez, A.M. Urtiaga, I. Ortiz, Assessment of the formation of inorganic oxidation by-products during the electrocatalytic treatment of ammonium from landfill leachates, Water Res. 46 (2012) 2579–2590. https://doi.org/10.1016/j.watres.2012.02.015.

[54] D. Landolt, N. Ibl, On the mechanism of anodic chlorate formation in concentrated NaCl solutions, Electrochimica Acta. 15 (1970) 1165–1183. https://doi.org/10.1016/0013-4686(70)85010-1.

[55] Y.J. Jung, K.W. Baek, B.S. Oh, J.-W. Kang, An investigation of the formation of chlorate and perchlorate during electrolysis using Pt/Ti electrodes: The effects of pH and reactive oxygen species and the results of kinetic studies, Water Research. 44 (2010) 5345–5355. https://doi.org/10.1016/j.watres.2010.06.029.